Rhodium and Iridium Amides

Michael D. Fryzuk,*[1] Patricia A. MacNeil, and Steven J. Rettig[2]

Department of Chemistry, University of British Columbia, Vancouver, British Columbia, Canada V6T 1Y6

Received February 7, 1986

A series of Rh(I) and Ir(I) amide complexes has been prepared and characterized; all of these M(L)[$N(SiMe_2CH_2PR_2)_2$] (M = Rh, Ir; L = C_8H_{14}, C_2H_4, CO, PMe_3, PPh_3) species are square-planar with the tridentate amide ligand phosphine donors in a mutually trans disposition. Oxidative addition of CH_3I or CH_3Br to the M(I) cyclooctene amides results in five-coordinate M(III) derivatives M(CH_3)X[$N(SiMe_2CH_2PR_2)_2$] (M = Rh, Ir; X = I, Br; R = Ph, *i*-Pr). On the basis of nOe difference ^1H NMR experiments and crystallographic data, these M(III) amides are thought to have a square-pyramidal stereochemistry both in the solid state and in solution. Monoclinic Ir(CH_3)I[$N(SiMe_2CH_2P(i\text{-}Pr)_2)_2$] crystallizes in the $P2_1/m$ space group with Z = 2, a = 9.6295 (7) Å, b = 15.2327 (5) Å, and c = 10.4068 (8) (Å); R_w = 0.029. Spectroscopic information regarding the CO adducts M(CO)(CH_3)X[$N(SiMe_2CH_2PR_2)_2$], formed by exposure to the M(III) amides to carbon monoxide under ambient conditions, indicates that the five-coordinate complexes maintain their square-pyramidal stereochemistry in solution.

Amide complexes of rhodium ($Rh(NR_2)L_n$) were totally unknown until Lappert's group reported[3] the synthesis of $Rh[N(SiMe_3)_2](PPh_3)_2$ in 1979. Moreover, in that original paper it was pointed out that amide derivatives of Tc, Os, Pd, and Ir were still unknown. We were so intrigued by the relatively few[4-6] complexes of the later transition elements containing the amide ligand that we initiated a study of their synthesis, structure, and reactivity patterns.

We have shown in earlier work[7,8] that incorporation of the amide donor NR_2^- (R = silyl) into a chelating array that contains phosphine donors allows for the preparation of group 10 (Ni triad) metal amides, in particular the first palladium amide complexes. Extension of this strategy to group 9 proved to be straightforward, allowing for the isolation[9] of a number of Rh(I) and Ir(I) amide derivatives of the general formula M(L)[$N(SiMe_2CH_2PR_2)_2$] (M = Rh, Ir; L = neutral ligand; R = Ph, *i*-Pr); the reactivity of these species with dihydrogen as well as their use as catalyst precursors in the homogeneous hydrogenation of 1-hexene have been the focus of earlier communications.[9-11] In this paper, we report full details of the synthesis and characterization of amide derivatives of rhodium(I) and iridium(I) and their reactivity with methyl halides to generate organometallic derivatives of rhodium(III) and iridium(III) stabilized by a disilylamide donor incorporated into a tridentate ligand system.

Experimental Section

General Information. All manipulations were performed under prepurified nitrogen in a Vacuum Atmospheres HE-553-2 glovebox equipped with a MO-40-2H purifier or in standard Schlenk-type glassware on a vacuum line. Both $RhCl_3.xH_2O$ and $IrCl_3.xH_2O$ were obtained from Johnson-Matthey and used as received to prepare $[Rh(\eta^2\text{-}C_8H_{14})_2Cl]_2$,[12] $[Ir(\eta^2\text{-}C_8H_{14})_2Cl]_2$[12] ($C_8H_{14}$ ≡ cyclooctene), $[Rh(CO)_2Cl]_2$,[13] $Rh(CO)_2Cl]_2$,[13] $[Rh(\eta^2\text{-}C_2H_4)_2Cl]_2$,[14] $Rh(PMe_3)_4Cl$,[15] and $Rh(PPh_3)_3Cl$[16] by the indicated literature procedures. The synthesis of the ligands LiN($SiMe_2CH_2PPh_2)_2$[8] and LiN($SiMe_2CH_2P(i\text{-}Pr)_2)_2$[17] was as reported earlier.

Toluene and diethyl ether (Et_2O) were purified by refluxing over dark blue or purple solutions of sodium–benzophenone ketyl (Na–Ph_2CO) followed by distillation under argon. Tetrahydrofuran (THF) and hexanes were predried by refluxing over CaH_2 and then distilled from Na–Ph_2CO under argon. Deuterated benzene (C_6D_6) and deuterated toluene (C_7D_8) were purchased from Aldrich, dried over activated 4-Å molecular sieves, and vacuum transferred prior to use.

Melting points were determined on a Mel-Temp apparatus in sealed capillaries under nitrogen and are uncorrected. Carbon, hydrogen, and nitrogen analyses of these air- and moisture-sensitive compounds were expertly performed by Mr. Peter Borda of this department. Infrared spectra were recorded either on a Pye-Unicam SP-1100 or a Nicolet 5D-X as KBr disks or in solution. ^1H NMR spectra were run on a Bruker WH-400 (400 MHz); $^{31}P\{^1H\}$ NMR spectra were recorded on a Bruker WP-80 (32.442 MHz) in 10-mm tubes and were referenced to external $P(OMe)_3$ set at +141.0 ppm relative to 85% H_3PO_4.

All reagents were obtained in the highest purity possible. Handling of gaseous reagents (CH_3Br, CH_3Cl, C_2H_4, and CO) was carried out on an all-glass vacuum line by using Hg manometers.

M(η^2-C_8H_{14})[$N(SiMe_2CH_2PR_2)_2$]. A solution of LiN($SiMe_2CH_2PR_2)_2$ (5 mmol) in toluene (50 mL) was added dropwise with stirring to a cold (−10 °C) solution of $[M(\eta^2\text{-}C_8H_{14})_2Cl]_2$ (2.5 mmol) in toluene (200 mL). The original clear orange solution darkened slightly during the addition. The solution was allowed to come to room temperature and then stirred at room temperature for 1 h. Removal of solvent yielded an oily residue which was extracted with hexanes, filtered through Celite, and pumped to dryness. Crystallization from minimum hexanes gave orange crystals which were washed with ~10 mL of cold (−30 °C) hexanes; yield 60–70%.

Rh(η^2-C_8H_{14})[$N(SiMe_2CH_2PPh_2)_2$] (1): $^{31}P\{^1H\}$ NMR (C_6D_6, 50 °C) 31.93 ppm (br d, $^1J_{Rh}$ = 140.4 Hz); mp 188–191 °C. Anal.

(1) Fellow of the Alfred P. Sloan Foundation (1984–1986).
(2) Experimental Officer: U.B.C. Crystal Structure Service
(3) Cetinkaya, B.; Lappert, M. F.; Torroni, S. *J. Chem. Soc., Chem. Commun.* **1979**, 843–844.
(4) Lappert, M. F.; Power, P. P.; Sanger, A. R.; Srivastava, R. C. *Metal and Metalloid Amides*, Horwood-Wiley: New York, 1980; p 485.
(5) (a) Bryndza, H. E.; Fultz, W. C.; Tam, W. *Organometallics* **1985**, *4*, 939–940. (b) Mainz, V. V.; Andersen, R. A. *Organometallics* **1984**, *3*, 675–678.
(6) Heddon, D.; Roundhill, D. M.; Fultz, W. C.; Rheingold, A. L. *J. Am. Chem. Soc.* **1984**, *106*, 5014–5016.
(7) Fryzuk, M. D.; MacNeil, P. A. *J. Am. Chem. Soc.* **1981**, *103*, 3592–3593.
(8) Fryzuk, M. D.; MacNeil, P. A.; Rettig, S. J.; Secco, A. S.; Trotter, J. *Organometallics* **1982**, *1*, 918–930.
(9) Fryzuk, M. D.; MacNeil, P. A. *Organometallics* **1983**, *2*, 355–356.
(10) Fryzuk, M. D.; MacNeil, P. A. *Organometallics* **1983**, *2*, 682–684.
(11) Fryzuk, M. D.; MacNeil, P. A.; Rettig, S. J. *Organometallics* **1985**, *4*, 1145–1147.
(12) Van der Ent, A.; Onderlinden, A. L. *Inorg. Synth.* **1973**, *14*, 93–95.
(13) McCleverty, J. A.; Wilkinson, G. *Inorg. Synth.* **1966**, *8*, 211–213.
(14) Cramer, R. *Inorg. Chem.* **1962**, *1*, 722–723.
(15) Jones, R. A.; Real, F. M.; Wilkinson, G.; Galas, A. M. R.; Hursthouse, M. B.; Malik, K. M. A. *J. Chem. Soc. Dalton Trans.* **1980**, 511–518.
(16) Jardin, F. H.; Osborn, J. A.; Wilkinson, G.; Young, J. F. *J. Chem. Soc. A* **1966**, 1711–1732.
(17) Fryzuk, M. D.; Carter, A.; Westerhaus, A. *Inorg. Chem.* **1985**, *24*, 642–648.

0276-7333/86/2305-2469$01.50/0

Calcd for $C_{38}H_{50}NP_2RhSi_2$: C, 61.54; H, 6.75; N, 1.89. Found: C, 61.33; H, 6.66; N, 1.87.

Ir(η^2-C_8H_{14})[N(SiMe$_2$CH$_2$PPh$_2$)$_2$] (6): $^{31}P\{^1H\}$ NMR (C_6D_6) 18.95 ppm (s, br). Anal. Calcd for $C_{38}H_{50}IrNP_2Si_2$: C, 54.94; H, 6.02; N, 1.69. Found: C, 54.78; H, 6.13; N, 1.59.

Rh(η^2-C_8H_{14})[N(SiMe$_2$CH$_2$P(*i*-Pr)$_2$)$_2$] (11). $^{31}P\{^1H\}$ NMR (C_6D_6) 35.1 ppm (br, m). Anal. Calcd for $C_{26}H_{58}NP_2RhSi_2$: C, 51.55; H, 9.65; N, 2.31. Found: C, 51.61; H, 9.70; N, 2.40.

Ir(η^2-C_8H_{14})[N(SiMe$_2$CH$_2$P(*i*-Pr)$_2$)$_2$] (12): $^{31}P\{^1H\}$ NMR (C_6D_6) 23.61 ppm (m). Anal. Calcd for $C_{26}H_{58}IrNP_2Si_2$: C, 44.93; H, 8.41; N, 2.02. Found: C, 44.73; H, 8.22; N, 1.97.

Rh(CO)[N(SiMe$_2$CH$_2$PPh$_2$)$_2$] (3). Method 1. To a cold (−78 °C) solution of $[Rh(CO)_2Cl]_2$ (0.20 g, 0.50 mmol) in Et_2O (60 mL) was added, dropwise with stirring, a solution of LiN(SiMe$_2$CH$_2$PPh$_2$)$_2$ (0.53 g, 1.0 mmol) in Et_2O (10 mL). The mixture was stirred at −78 °C for 30 min, warmed to 0 °C for an hour, and finally stirred at room temperature for 2 h. The originally clear yellow solution deepened to a murky orange during the course of this reaction. The solvent was then removed in vacuo and the residue extracted with hexanes, filtered, and pumped to dryness. The product was recrystallized as yellow-orange needles from hexanes: yield 0.47 g (71%); mp 128–130 °C; IR (CH_2Cl_2) ν_{CO} 1950 cm^{-1} (vs); $^{31}P\{^1H\}$ NMR (C_6D_6) 30.92 ppm (d, $^1J_{Rh}$ = 129.4 Hz). Anal. Calcd for $C_{31}H_{36}NOP_2RhSi_2$: C, 56.45; H, 5.46; N, 2.12. Found: C, 56.70; H, 5.50; N, 2.01.

Method 2. A solution of Rh(η^2-C_8H_{14})[N(SiMe$_2$CH$_2$PPh$_2$)$_2$] (0.12 g, 0.20 mmol) in toluene (20 mL) was stirred under 1 atm of CO at room temperature for 30 min. During this time period, the original gold solution lightened rapidly to a clear yellow. The solvent was removed and the oily residue recrystallized from hexanes; yield 90%.

Rh(η^2-C_2H_4)[N(SiMe$_2$CH$_2$PPh$_2$)$_2$] (2). This complex was prepared by either method 1, using $[Rh(\eta^2\text{-}C_2H_4)_2Cl]_2$ in Et_2O, or method 2, from Rh(η^2-C_8H_{14})[N(SiMe$_2$CH$_2$PPh$_2$)$_2$] in toluene under 1 atm of C_2H_4. The reaction conditions and workup procedures for both methods were as described for the carbonyl derivative: yield, method 1, 70%, method 2, 83%; mp 156–158 °C; $^{31}P\{^1H\}$ NMR (C_6D_6) 32.48 ppm (d, $^1J_{Rh}$ = 131.8 Hz). Anal. Calcd for $C_{32}H_{40}NP_2RhSi_2$: C, 58.27; H, 6.07; N, 2.12. Found: C, 58.55; H, 5.95; N, 2.09.

Rh(PMe$_3$)[N(SiMe$_2$CH$_2$PPh$_2$)$_2$] (5). Synthesis of this derivative was carried out by using $Rh(PMe_3)_4Cl$ in Et_2O (method 1); alternatively, this complex was more easily prepared via method 2, using a slight excess of PMe_3, added to a toluene solution of Rh(η^2-C_8H_{14})[N(SiMe$_2$CH$_2$PPh$_2$)$_2$]: yield, method 1, 68%, method 2, 92%; mp 225–227 °C; $^{31}P\{^1H\}$ NMR (C_6D_6), PPh$_2$, 33.42 (dd, $^1J_{Rh}$ = 144.3, $^2J_{PPh_2,PMe_3}$ = 44.4 Hz), PMe$_3$, −10.26 ppm (dt, $^1J_{Rh}$ = 148.0 Hz). Anal. Calcd for $C_{33}H_{45}NP_3RhSi_2$: C, 56.01: H, 6.36; N, 1.98. Found: C, 56.35; H, 6.40; N, 1.91.

Rh(PPh$_3$)[N(SiMe$_2$CH$_2$PPh$_2$)$_2$] (4). This complex was prepared via method 1, from Wilkinson's catalyst, $Rh(PPh_3)_3Cl$, in THF, or by means of method 2, from Rh(η^2-C_8H_{14})[N(SiMe$_2$CH$_2$PPh$_2$)$_2$] and 1 equiv of recrystallized PPh_3 in toluene. The latter transformation requires 2 days at room temperature to go to completion: yield, method 1, 63%, method 2, 86%; mp 172–174 °C; $^{31}P\{^1H\}$ NMR (C_6D_6), PPh$_3$, 50.00 (dt, $^1J_{Rh}$ = 163.6, $^2J_{PPh_2,PPh_3}$ = 40.3 Hz), PPh$_2$, 31.94 ppm (dd, $^1J_{Rh}$ = 142.8 Hz). Anal. Calcd for $C_{48}H_{51}NP_3RhSi_2$: C, 64.50; H, 5.71; N, 1.57. Found: C, 64.83; H, 5.60; N, 1.49.

Ir(η^2-C_2H_4)[N(SiMe$_2$CH$_2$PPh$_2$)$_2$] (7). Preparation of this derivative was as outlined for its rhodium analogue (method 2 only): yield 74%; $^{31}P\{^1H\}$ NMR (C_6D_6) 21.95 ppm (s). Anal. Calcd for $C_{32}H_{40}IrNP_2Si_2$: C, 51.34; H, 5.35; N, 1.87. Found: C, 51.43; H, 5.45; N, 1.93.

Ir(PMe$_3$)[N(SiMe$_2$CH$_2$PPh$_2$)$_2$] (10). The synthesis of this complex was carried out as described for its rhodium analogue (method 2): yield 82%; $^{31}P\{^1H\}$ NMR (C_6D_6), PPh$_2$, 24.10 (d, $^2J_{PPh_2,PMe_3}$ = 28.4 Hz), PMe$_3$, −51.17 ppm (t). Anal. Calcd for $C_{33}H_{45}IrNP_3Si_2$: C, 49.75; H, 5.65; N, 1.76. Found: C, 49.77; H, 5.78; N, 1.68.

Ir(PPh$_3$)[N(SiMe$_2$CH$_2$PPh$_2$)$_2$] (9). A solution of Ir(η^2-C_8H_{14})[N(SiMe$_2$CH$_2$PPh$_2$)$_2$] (0.17 g, 0.2 mmol) and freshly recrystallized triphenylphosphine (52 mg, 0.2 mmole) in toluene (30 mL) was refluxed over 24 h under nitrogen. The deep orange solution was then allowed to cool to room temperature and the solvent removed in vacuo. Recrystallization from neat hexane yielded analytically pure orange needles: yield 0.15 g (78%); $^{31}P\{^1H\}$ NMR (C_6D_6), PPh$_2$, 23.72 (d, $^2J_{PPh_2,PPh_3}$ = 22.0 Hz), PPh$_3$, 19.71 ppm (t). Anal. Calcd for $C_{48}H_{51}IrNP_3Si_2$: C, 58.66; H, 5.19; N, 1.42. Found: C, 58.74; H, 5.20; N, 1.34.

Ir(CO)[N(SiMe$_2$CH$_2$PPh$_2$)$_2$] (8). This complex was prepared in an identical fashion to that described for its rhodium analogue (method 2 only) from Ir(η^2-C_8H_{14})[N(SiMe$_2$CH$_2$PPh$_2$)$_2$] in toluene under 1 atm CO: yield 95%; mp 138–139 °C; IR (CH_2Cl_2) ν_{CO} 1930 cm^{-1} (vs); $^{31}P\{^1H\}$ NMR (C_6D_6) 23.94 ppm (s). Anal. Calcd for $C_{31}H_{36}IrNOP_2Si_2$: C, 49.73; H, 4.81; N, 1.87. Found: C, 49.96; H, 5.00; N, 1.76.

M(CH$_3$)I[N(SiMe$_2$CH$_2$PR$_2$)$_2$]. Preparation of the above compounds (M = Rh, Ir; R = Ph, *i*-Pr) involved vacuum transfer at −10 °C of an excess (at least 10-fold) of methyl iodide, which had been previously freeze–pump–thawed for several cycles, to a toluene (50-mL) solution of the cyclooctene complex M(η^2-C_8H_{14})[N(SiMe$_2$CH$_2$PR$_2$)$_2$] (~1 g). The solution was allowed to warm to room temperature, during which time the original orange color changed to either deep emerald green (M = Ir, R = Ph), blue-green (M = Ir, R = *i*-Pr), green-blue (M = Rh, R = Ph), or purple (M = Rh, R = *i*-Pr). Typical reaction times were 1–5 h. Solvent removal followed by crystallization from hexanes yielded crystalline products; yield 80–90%.

Ir(CH$_3$)I[N(SiMe$_2$CH$_2$PPh$_2$)$_2$] (14): $^{31}P\{^1H\}$ NMR (C_6D_6) 10.11 ppm (s); molecular weight (Signer), calcd 862, found 864. Anal. Calcd for $C_{31}H_{39}IIrNP_2Si_2$: C, 43.15; H, 4.56; N, 1.62. Found: C, 43.28; H, 4.64; N, 1.69.

Ir(CH$_3$)I[N(SiMe$_2$CH$_2$P(*i*-Pr)$_2$)$_2$] (16): $^{31}P\{^1H\}$ NMR (C_6D_6) 15.78 ppm (s); molecular weight (Signer), calcd 726, found 675. Anal. Calcd for $C_{19}H_{47}IIrNSi_2P_2$: C, 31.40; H, 6.52; N, 1.93. Found: C, 31.70; H, 6.50; N, 1.92.

Rh(CH$_3$)I[N(SiMe$_2$CH$_2$PPh$_2$)$_2$] (13): $^{31}P\{^1H\}$ NMR (C_6D_6) 25.00 ppm (d, $^1J_{Rh}$ = 107.4 Hz). Anal. Calcd for $C_{31}H_{39}INP_2RhSi_2$: C, 48.13; H, 5.08; N, 1.81. Found: C, 47.93; H, 5.25; N, 1.70.

Rh(CH$_3$)I[N(SiMe$_2$CH$_2$P(*i*-Pr)$_2$)$_2$] (15): $^{31}P\{^1H\}$ NMR (C_6D_6) 34.97 ppm (d, $^1J_{Rh}$ = 122.6 Hz). Anal. Calcd for $C_{19}H_{47}INPRhSi_2$: C, 35.80; H, 7.43; N, 2.20. Found: C, 36.10; H, 7.40; N, 2.27.

M(CH$_3$)Br[N(SiMe$_2$CH$_2$PPh$_2$)$_2$]. An excess of reagent grade CH_3Br (~30 equiv) was freeze–pump–thawed several times prior to vacuum transfer at −10 °C to a toluene solution (50 mL) of M(η^2-C_8H_{14})[N(SiMe$_2$CH$_2$PPh$_2$)$_2$] (~1 g). Over a 1 h period, the solution gradually became green (M = Ir) or blue (M = Rh) in color; stirring at room temperature was continued overnight. Solvent removal followed by crystallization from toluene/hexanes yielded deep blue-green crystals of the iridium complex or black-blue crystals of the rhodium analogue.

Ir(CH$_3$)Br[N(SiMe$_2$CH$_2$PPh$_2$)$_2$] (18): $^{31}P\{^1H\}$ NMR (C_6D_6) 9.31 ppm (s). Anal. Calcd for $C_{31}H_{39}BrIrNP_2Si_2$: C, 45.64; H, 4.82; N, 1.72. Found: C, 45.63; H, 4.80; N, 1.66.

Rh(CH$_3$)Br[N(SiMe$_2$CH$_2$PPh$_2$)$_2$] (17): $^{31}P\{^1H\}$ NMR (C_6D_6) 22.47 ppm (d, $^1J_{Rh}$ = 107.4 Hz). Anal. Calcd for $C_{31}H_{39}BrNP_2RhSi_2$: C, 51.24; H, 5.41; N, 1.93. Found: C, 51.50; H, 5.51; N, 2.00.

M(CH$_3$)I(CO)[N(SiMe$_2$CH$_2$PR$_2$)$_2$]. All reactions were carried out in toluene at room temperature by allowing a solution of M(CH$_3$)I[N(SiMe$_2$CH$_2$PR$_2$)$_2$] to stir under 1 atm of CO. Within minutes, a dramatic color change occurred to give pale yellow to orange solutions. Upon solvent removal the iridium complexes were obtained as pale yellow (R = Ph) or orange-yellow (R = *i*-Pr) crystals. The analogous rhodium complexes are less stable, losing coordinated CO when exposed to vacuum. Accordingly, ^1H NMR and IR data were obtained under an atmosphere of CO. If the reaction is carried out in hexanes, orange crystals of the rhodium carbonyls can be obtained at −10 °C, but, even in the solid state these derivatives rapidly decompose at room temperature under vacuum.

Ir(CH$_3$)I(CO)[N(SiMe$_2$CH$_2$PPh$_2$)$_2$] (19): IR (KBr) ν_{CO} 2020 cm^{-1} (vs); $^{31}P\{^1H\}$ NMR (C_6D_6) −17.04 ppm (s). Anal. Calcd for $C_{32}H_{39}IIrNOP_2Si_2$: C, 43.14; H, 4.41; N, 1.57. Found: C, 42.90; H, 4.47; N, 1.48.

Ir(CH$_3$)I(CO)[N(SiMe$_2$CH$_2$P(*i*-Pr)$_2$)$_2$] (20): IR (KBr) ν_{CO} 2005 cm^{-1} (vs); $^{31}P\{^1H\}$ NMR (C_6D_6) −2.28 ppm (s). Anal. Calcd for $C_{20}H_{47}IIrNOP_2Si_2$: C, 31.82; H, 6.28; N, 1.86. Found: C, 32.08; H, 6.49; N, 1.79.

Table I. ^{1}H NMR Spectral Data[a]

complex	$Si(CH_3)_2$	PCH_2Si	$P(C_6H_5)_2$	other	
$Rh(\eta^2\text{-}C_8H_{14})[N(SiMe_2CH_2PPh_2)_2]$	0.10 (s)	1.77 (t, J_{app} = 4.2)	7.09 (m, para/meta) 7.82 (m, ortho)	C_8H_{14}	1.22 (br m), 2.21 (br m), 2.79 (br m)
$Rh(\eta^2\text{-}C_2H_4)[N(SiMe_2CH_2PPh_2)_2]$	0.26 (s)	1.78 (t, J_{app} = 4.5)	7.11 (m, para/meta) 7.78 (m, ortho)	C_2H_4	2.24 (dt, $^2J_{Rh}$ = 1.8, ^3J_P = 4.0)
$Rh(CO)[N(SiMe_2CH_2PPh_2)_2]$	0.22 (s)	1.73 (t, J_{app} = 5.0)	7.02 (m, para/meta) 7.82 (m, ortho)		
$Rh(PPh_3)[N(SiMe_2CH_2PPh_2)_2]$	0.24 (s)	1.92 (t, J_{app} = 4.1)	7.00 (m, para/meta) 7.66 (m, ortho)	$P(C_6H_5)_3$	6.86 (m)
$Rh(PMe_3)[N(SiMe_2CH_2PPh_2)_2]$	0.11 (s)	1.82 (t, J_{app} = 4.8)	7.10 (m, para/meta) 7.99 (m, ortho)	$P(CH_3)_3$	0.62 (dd, ^2J_P = 8.1, $^3J_{Rh}$ = 1.0)
$Ir(\eta^2\text{-}C_8H_{14})[N(SiMe_2CH_2PPh_2)_2]$[b]	0.10 (s)	1.80 (t, J_{app} = 4.2)	7.08 (m, para/meta) 7.82 (m, ortho)	C_8H_{14}	1.25 (br m), 2.15 (br m)
$Ir(\eta^2\text{-}C_2H_4)[N(SiMe_2CH_2PPh_2)_2]$	0.18 (s)	1.76 (t, J_{app} = 5.2)	7.02 (m, para/meta) 7.72 (m, ortho)	C_2H_4	1.34 (t, ^3J_P = 5.0)
$Ir(CO)[N(SiMe_2CH_2PPh_2)_2]$	0.20 (s)	1.78 (t, J_{app} = 5.9)	7.00 (m, para/meta) 7.95 (m, ortho)		
$Ir(PPh_3)[N(SiMe_2CH_2PPh_2)_2]$	0.20 (s)	1.82 (t, J_{app} = 4.5)	6.93 (m, para/meta) 7.65 (m, ortho)	$P(C_6H_5)_3$	6.76 (m)
$Ir(PMe_3)[N(SiMe_2CH_2PPh_2)_2]$	0.15 (s)	1.82 (t, J_{app} = 5.0)	7.07 (m, para/meta) 8.07 (m, ortho)	$P(CH_3)_3$	0.80 (d, ^2J_P = 8.6)
$Rh(\eta^2\text{-}C_8H_{14})[N(SiMe_2CH_2P(i\text{-}Pr)_2)_2]$	0.40 (s)	0.62 (t, J_{app} = 4.5)		$P(CH(CH_3)_2)_2$ $P(CH(CH_3)_2)_2$ C_8H_{14}	1.18 (m) 2.04 (m) 1.58 (br m), 2.35 (br m)
$Ir(\eta^2\text{-}C_8H_{14})[N(SiMe_2CH_2P(i\text{-}Pr)_2)_2]$	0.38 (s)	0.96 (t, J_{app} = 6.5)		$P(CH(CH_3)_2)_2$ C_8H_{14}	1.26 (br m) 1.30 (br m), 2.25 (br m)
$Rh(CH_3)I[N(SiMe_2CH_2PPh_2)_2]$	−0.22 (s) 0.42 (s)	1.58 (dt, J_{app} = 5.4, $^2J_{gem}$ = 13.5) 1.76 (dt, J_{apo} = 5.0)	7.08 (m, para/meta) 7.74 (m, ortho) 7.91 (m, ortho)	$RhCH_3$	1.69 (dt, $^2J_{Rh}$ = 3.0, ^3J_P = 8.0)
$Ir(CH_3)I[N(SiMe_2CH_2PPh_2)_2]$	−0.13 (s) 0.44 (s)	1.64 (q of t, J_{app} = 5.5)	7.07 (m, para/meta) 7.73 (m, ortho) 7.78 (m, ortho)	$IrCH_3$	2.02 (t, ^3J_P = 6.0)
$Rh(CH_3)I[N(SiMe_2CH_2P(i\text{-}Pr)_2)_2]$	0.28 (s)	0.81 (t, J_{app} = 5.1)		$RhCH_3$	1.99 (dt, $^2J_{Rh}$ = 3.0, ^3J_P = 5.8)
	0.31 (s)			$P(CH(CH_3)_2)_2$ $P(CH(CH_3)_2)_2$	1.11 (m) 2.57 (m)
$Ir(CH_3)I[N(SiMe_2CH_2P(i\text{-}Pr)_2)_2]$	0.42 (s) 0.43 (s)	0.85 (t, J_{app} = 5.2)		$IrCH_3$ $P(CH(CH_3)_2)_2$ $P(CH(CH_3)_2)_2$	2.42 (t, ^3J_P = 4.8) 1.10 (m) 2.77 (m)
$Rh(CH_3)Br[N(SiMe_2CH_2PPh_2)_2]$	−0.13 (s) 0.39 (s)	1.53 (dt, J_{app} = 5.6, $^2J_{gem}$ = 14.9) 1.64 (dt, J_{app} = 5.1)	7.07 (m, para/meta) 7.86 (m, ortho) 7.97 (m, ortho)	$RhCH_3$	1.75 (dt, $^2J_{Rh}$ = 2.7, ^3J_P = 6.3)
$Ir(CH_3)Br[N(SiMe_2CH_2PPh_2)_2]$	−0.10 (s) 0.41 (s)	1.57 (t, J_{app} = 5.5)	7.07 (m, para/meta) 7.84 (m, ortho) 7.96 (m, ortho)	$IrCH_3$	2.03 (t, ^3J_P = 6.2)
$Ir(CH_3)I(CO)[N(SiMe_2CH_2PPh_2)_2]$ (19)	0.04 (s) 0.47 (s)	1.65 (dt, J_{app} = 6.1, $^2J_{gem}$ = 13.8) 1.90 (dt, J_{app} = 7.0)	7.03 (m, para/meta) 7.76 (m, ortho) 8.14 (m, ortho)	$IrCH_3$	0.95 (t, ^3J_P = 9.0)
$Ir(CH_3)I(CO)[N(SiMe_2CH_2P(i\text{-}Pr)_2)_2]$	0.26 (s) 0.35 (s)	1.11 (m)		$IrCH_3$ $P(CH(CH_3)_2)_2$ $P(CH(CH_3)_2)_2$	1.11 (obscured) 1.11 (obscured) 2.43 (m), 2.80 (m)
$Rh(CH_3)I(CO)[N(SiMe_2CH_2PPh_2)_2]$	0.01 (s) 0.42 (s)	1.62 (dt, J_{app} = 6.3, $^2J_{gem}$ = 13.2) 1.86 (dt, J_{app} = 6.5)	7.04 (m, para/meta) 7.78 (m, ortho) 8.14 (m, ortho)	$RhCH_3$	1.11 (dt, $^2J_{Rh}$ = 2.0, ^3J_P = 7.8)
$Rh(CH_3)I(CO)[N(SiMe_2CH_2P(i\text{-}Pr)_2)_2]$	0.26 (s)	1.12 (m)		$RhCH_3$	1.35 (dt, $^2J_{Rh}$ = 2.4, ^3J_P = 6.6)
	0.33 (s)			$P(CH(CH_3)_2)_2$ $P(CH(CH_3)_2)_2$	1.18 (m) 2.40 (m), 2.76 (m)
$Ir(CH_3)I(CO)[N(SiMe_2CH_2PPh_2)_2]$ (23)	0.38 (s) 0.70 (s)	2.16 (dt, J_{app} = 5.0, $^2J_{gem}$ = 13.8) 2.47 (dt, J_{app} = 7.6)	6.95 (m, para/meta) 7.08 (m, para/meta) 7.43 (m, ortho) 8.03 (m, ortho)	$IrCH_3$	0.58 (t, ^3J_P = 6.5)

[a] All spectra recorded at 25 °C unless specified otherwise. All spectra were recorded in C_6D_6 at 400 MHz and referenced to C_6H_5H at 7.15 ppm; all J values are given in hertz. [b] This spectrum recorded at 50 °C.

$Rh(CH_3)I(CO)[N(SiMe_2CH_2PPh_2)_2]$ (21): IR (KBr) ν_{CO} 2055 cm^{-1} (vs); $^{31}P\{^1H\}$ NMR (C_6D_6) 20.63 ppm (d, $^1J_{Rh}$ = 95.2 Hz).

$Rh(CH_3)I(CO)[N(SiMe_2CH_2P(i\text{-}Pr)_2)_2]$ (22): IR (KBr) ν_{CO} 2035 cm^{-1} (vs); $^{31}P\{^1H\}$ NMR (C_6D_6) 35.13 ppm (d, $^1J_{Rh}$ = 87.9 Hz).

$Ir(CH_3)I(CO)[N(SiMe_2CH_2PPh)_2]$ (23): To a toluene solution (20 mL) of $Ir(CO)[N(SiMe_2CH_2PPh_2)_2]$ (150 mg, 0.20 mmol) was vacuum transferred, from a −10 °C bath, an excess of methyl iodide (~50 equiv). Upon warming to room temperature, the solution rapidly decolorized. Solvent removal followed by crystallization from toluene/hexanes yielded almost colorless needles of **23**: yield 145 mg (85%); IR (KBr) ν_{CO} 1988 cm^{-1} (vs); $^{31}P\{^1H\}$ NMR (C_6D_6) 3.92 ppm (s). Anal. Calcd for $C_{32}H_{39}IIrNOP_2Si_2$: C, 43.14; H, 4.41; N, 1.57. Found: C, 43.40; H, 4.55; N, 1.68.

X-ray Crystallographic Analysis of $Ir(CH_3)I[N(SiMe_2CH_2P(i\text{-}Pr)_2)_2]$. Crystallographic data appear in Table II. Final unit-cell parameters were obtained by least-squares on (2 sin θ)/λ values for 25 reflections, measured with Mo $K\alpha_1$ radiation. The intensities of 3 check reflections, measured each hour of X-ray exposure time throughout the data collection, decreased uniformly by about 5%. The data were scaled accordingly, and an absorption correction was applied by using the

Table II. Crystallographic Data[a]

compd	$[(i\text{-}Pr_2PCH_2SiMe_2)_2N]MeIrI$
formula	$C_{19}H_{47}IIrNP_2Si_2$
fw	726.83
cryst system	monoclinic
space group	$P2_1/m$
a, Å	9.6295 (7)
b, Å	15.2327 (5)
c, Å	10.4068 (8)
α, deg	90
β, deg	111.774 (4)
γ, deg	90
V, Å^3	1417.6 (2)
Z	2
D_{calcd}, g/cm^3	1.703
$F(000)$	712
μ(Mo Kα), cm^{-1}	59.7
crystal dimens, mm	0.13 × 0.38 × 0.57
transmissn factors	0.139–0.470
scan type	ω–2θ
scan range, deg in ω	0.70 + 0.35 tan θ
scan speed, deg/min	1.34–10.06
data collected	$+h,+k,\pm l$
$2\theta_{max}$, deg	60
unique reflctns	4266
reflctns with $I \geq 3\sigma(I)$	3342
no. of variables	223
R	0.026
R_w	0.029
S	1.144
mean Δ/σ (final cycle)	0.01
max Δ/σ (final cycle)	0.07
residual density, e/Å^3	−1.21 to 0.96

[a] Temperature 22 °C, Enraf-Nonius CAD4-F diffractometer, Mo Kα radiation ($\lambda_{K\alpha_1}$ = 0.709 30 Å; $\lambda_{K\alpha_2}$ = 0.713 59 Å); graphite monochromator; takeoff angle 2.7°; aperature (2.0 + tan θ) × 4.0 mm at a distance of 173 mm from the crystal; scan range extended by 25% on both sides for background measurement, $\sigma^2(I) = S + 2B + [0.04(S - B)]^2$ (S = scan count, B = normalized background count); function minimized $\sum w(|F_o| - |F_c|)^2$ where w ; $1/\sigma^2(F)$, $R = \sum||F_o| - |F_c||/\sum|F_o|$, $R_w = (\sum w(|F_o| - |F_c|)^2/\sum w|F_o|^2)^{1/2}$, and $S = (\sum w(|F_o| - |F_c|)^2/(m - n))^{1/2}$. Values given for R, R_w, and S are based on those reflections with $I \geq 3\sigma(I)$.

Gaussian integration method;[18-20] the range of transmission factors is given in Table II.

The systematic absences ($0k0$, k odd) allow space groups $P2_1$ and $P2_1/m$. The analysis was initiated in the noncentrosymmetric space group $P2_1$ on the basis of the number of molecules in the unit cell ($Z = 2$). The coordinates of the Ir, I, P, and Si atoms were determined from the Patterson function. A difference map showed large peaks corresponding to I, P, and Si positions mirrored across a plane containing the Ir atom and normal to the b axis. In subsequent stages of refinement the structure was assumed to be disordered 1:1 about the mirror plane in the centrosymmetric space group $P2_1/m$.

In the final stages of full-matrix least-square refinement all non-hydrogen atoms were refined with anisotropic thermal parameters and hydrogen atoms were included as fixed atoms in calculated positions (methyl H positions based on those observed on a difference map; C–H = 0.98 Å; $U_H \propto U$ parent). Three isopropyl carbon atoms (C(4), C(12), and C(17)) were found to lie on the mirror plane, but, on the basis of the thermal parameters, it is likely that these atoms are slightly displaced from the mirror plane. Attempts to refine the y coordinate of these carbon atoms were not successful, presumably because the maximum electron density occurs at $y = {}^1/_4$ since the separation of the two mirror-related half atoms is too small to resolve. A result of this deficiency in the model is apparent shortening of the C(4)–C(13) and C(6)–C(17) bonds.

Neutral atom scattering factors and anomalous scattering corrections (Ir, I, P, and Si) were taken from ref 21. Final positional and equivalent isotropic thermal parameters (U_{eq} = ${}^1/_3$ trace diagonalized U) for the non-hydrogen atoms are given in Table VIII. Bond lengths, bond angles, and intraannular torsion angles appear in Tables III, IV, and V, respectively. Anisotropic thermal parameters, calculated hydrogen atom parameters, and measured and calculated structure factor amplitudes are included as supplementary material (Tables VI, VII, IX).

Table III. Bond Lengths (Å) with Estimated Standard Deviations in Parentheses for $Ir(CH_3)I[N(SiMe_2CH_2P(i\text{-}Pr)_2)_2]$

Ir–I	2.6875 (5)	Si(1)–C(9)	1.872 (8)
Ir–P(1)	2.327 (2)	Si(2)–N	1.716 (6)
Ir–P(2)	2.335 (2)	Si(2)–C(2)	1.873 (9)
Ir–N	2.079 (5)	Si(2)–C(10)	1.863 (9)
Ir–C(3)	2.079 (7)	Si(2)–C(11)	1.879 (10)
P(1)–C(1)	1.814 (8)	C(4)–C(12)	1.527 (9)
P(1)–C(4)	1.870 (5)	C(4)–C(13)	1.439 (11)
P(1)–C(5)	1.861 (8)	C(5)–C(14)	1.498 (13)
P(2)–C(2)	1.810 (7)	C(5)–C(15)	1.516 (11)
P(2)–C(6)	1.845 (8)	C(6)–C(16)	1.564 (12)
P(2)–C(7)	1.853 (7)	C(6)–C(17)	1.427 (11)
Si(1)–N	1.725 (6)	C(7)–C(18)	1.530 (14)
Si(1)–C(1)	1.878 (8)	C(7)–C(19)	1.535 (12)
Si(1)–C(8)	1.873 (8)		

Table IV. Bond Angles (deg) with Estimated Standard Deviations in Parentheses for $Ir(CH_3)I[N(SiMe_2CH_2P(i\text{-}Pr)_2)_2]$

I–Ir–P(1)	91.28 (4)	C(1)–Si(1)–C(9)	108.5 (4)
I–Ir–P(2)	92.51 (4)	C(8)–Si(1)–C(9)	105.8 (5)
I–Ir–N	174.44 (15)	N–Si(2)–C(2)	107.8 (3)
I–Ir–C(3)	92.9 (3)	N–Si(2)–C(10)	114.8 (4)
P(1)–Ir–P(2)	170.02 (6)	N–Si(2)–C(11)	111.6 (4)
P(1)–Ir–N	85.95 (15)	C(2)–Si(2)–C(10)	106.3 (4)
P(1)–Ir–C(3)	95.1 (2)	C(2)–Si(2)–C(11)	109.1 (6)
P(2)–Ir–N	89.46 (15)	C(10)–Si(2)–C(11)	107.0 (6)
P(2)–Ir–C(3)	93.9 (2)	Ir–N–Si(1)	118.0 (3)
N–Ir–C(3)	92.1 (3)	Ir–N–Si(2)	118.5 (3)
Ir–P(1)–C(1)	107.9 (2)	Si(1)–N–Si(2)	123.3 (3)
Ir–P(1)–C(4)	109.63 (15)	P(1)–C(1)–Si(1)	110.1 (4)
Ir–P(1)–C(5)	123.4 (3)	P(2)–C(2)–Si(2)	111.9 (4)
C(1)–P(1)–C(4)	104.4 (3)	P(1)–C(4)–C(12)	112.2 (4)
C(1)–P(1)–C(5)	105.5 (4)	P(1)–C(4)–C(13)	114.0 (5)
C(4)–P(1)–C(5)	104.4 (3)	C(12)–C(4)–C(13)	109.1 (5)
Ir–P(2)–C(2)	107.9 (3)	P(1)–C(5)–C(14)	112.4 (5)
Ir–P(2)–C(6)	125.5 (3)	P(1)–C(5)–C(15)	112.9 (7)
Ir–P(2)–C(7)	109.9 (3)	C(14)–C(5)–C(15)	110.4 (8)
C(2)–P(2)–C(6)	104.0 (4)	P(2)–C(6)–C(16)	112.2 (7)
C(2)–P(2)–C(7)	106.0 (4)	P(2)–C(6)–C(17)	114.2 (6)
C(6)–P(2)–C(7)	102.1 (4)	C(16)–C(6)–C(17)	116.9 (8)
N–Si(1)–C(1)	107.1 (3)	P(2)–C(7)–C(18)	110.8 (6)
N–Si(1)–C(8)	114.3 (4)	P(2)–C(7)–C(19)	114.7 (7)
N–Si(1)–C(9)	113.2 (4)	C(18)–C(7)–C(19)	110.8 (8)
C(1)–Si(1)–C(8)	107.6 (4)		

Results and Discussion

Rh(I) and Ir(I) Amides. The reaction of a number of readily available rhodium(I) chloride derivatives with an equimolar amount of the lithium amide $LiN(SiMe_2CH_2PPh_2)_2$[8] in toluene at 0 °C generates a variety of neutral, monomeric amide complexes (eq 1).

For the synthesis of iridium(I) amides, the only suitable readily available starting material is the bis(cyclooctene) dimer $[Ir(\eta^2\text{-}C_8H_{14})_2Cl]_2$ which reacts analogously to the rhodium precursor (eq 1) to generate the corresponding iridium(I) derivative **6** (eq 2). All of these species, upon

(18) The computer programs used include locally written programs for data processing and locally modified versions of the following: ORFLS, full-matrix least-squares, and ORFFE, function and errors, by W. R. Busing, K. O. Martin, and H. A. Levy; FORDAP, Patterson and Fourier syntheses, by A. Zalkin; ORTEP II, illustrations, by C. K. Johnson.

(19) Coppens, P.; Leiserowitz, L.; Rabinovich, D. *Acta Crystallogr.* **1965**, *18*, 1035–1038.

(20) Busing, W. R.; Levy, H. A. *Acta Crystallogr.* **1967**, *22*, 457–464.

(21) *International Tables for X-ray Crystallography*; Kynoch Press: Birmingham, 1974; Vol. IV.

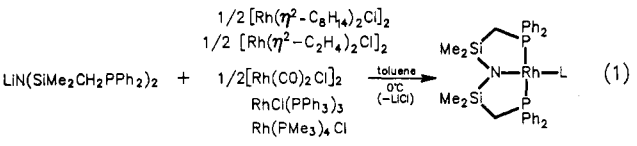

1: L = η^2-C_8H_{14}
2: L = η^2-C_2H_4
3: L = CO
4: L = PPh_3
5: L = PMe_3

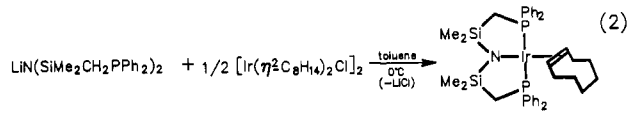

6

extraction with hexanes, can be isolated as air- and moisture-sensitive, yellow or orange crystalline solids; if stored under an inert atmosphere, these compounds are stable in the solid state for months at room temperature.

The most versatile amide derivatives of rhodium(I) and iridium(I) are the η^2-cyclooctene complexes **1** and **6** as they can be used to generate other amide species by displacement of the labile cyclooctene ligand by other neutral ligands (eq 3).

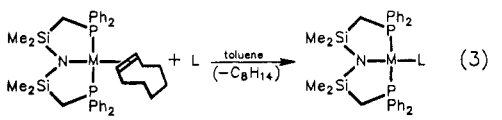

2: M = Rh; L = η^2-C_2H_4
3: M = Rh; L = CO
4: M = Rh; L = PPh_3
5: M = Rh; L = PMe_3
7: M = Ir; L = η^2-C_2H_4
8: M = Ir; L = CO
9: M = Ir; L = PPh_3
10: M = Ir; L = PMe_3

Extension of this strategy to other ligand derivatives containing isopropyl substituents at phosphorus is also straightforward; in these cases as above, the η^2-cyclooctene complexes are the derivatives of choice.

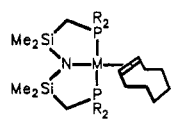

M	R	
Rh	i-Pr	11
Ir	i-Pr	12

Structural characterization of these species was based primarily on ^1H NMR spectral assignments (Table I), although the $^{31}P\{^1H\}$ NMR and IR spectra were also informative in obvious cases. With the exception of the η^2-cyclooctene complex **6**, all of the other neutral amide derivatives have a virtual triplet in the ^1H NMR spectrum at room temperature for the methylene protons (PCH_2Si) in the ligand backbone; as previously reported[8] for the related group 10 derivatives, this observation is consistent with a square-planar geometry having trans disposed phosphine donors. The iridium cyclooctene derivative **6** shows broadened resonances at ambient temperature in the ^1H NMR spectrum; when **6** is warmed to 50 °C, however, a sharpened spectrum comparable to the other cyclooctene complexes is obtained. Undoubtedly this behavior is due to restricted rotation of the η^2-cyclooctene ligand about the Ir–olefin bond on the ^1H NMR time scale.

Oxidative Addition of Methyl Halides. Not only are the cyclooctene complexes described above useful precursors to Rh(I) and Ir(I) adducts, but also they are excellent starting materials for the formation of Rh(III) and Ir(III) amide derivatives via oxidative addition of certain methyl halides. Thus the reaction of $M(\eta^2\text{-}C_8H_{14})[N(SiMe_2CH_2PR_2)_2]$ (M = Rh, Ir; R = Ph, *i*-Pr) with iodomethane results in the loss of cyclooctene and formation of five-coordinate methyl iodide adducts (eq 4). The

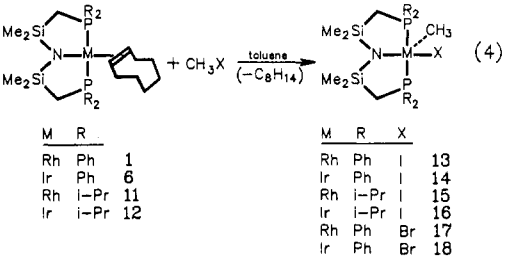

M	R	
Rh	Ph	1
Ir	Ph	6
Rh	i-Pr	11
Ir	i-Pr	12

M	R	X	
Rh	Ph	I	13
Ir	Ph	I	14
Rh	i-Pr	I	15
Ir	i-Pr	I	16
Rh	Ph	Br	17
Ir	Ph	Br	18

analogous reaction of excess bromomethane with the cyclooctene precursor complexes **1** and **6** generates the corresponding five-coordinate methyl bromide adducts **17** and **18**, respectively (eq 4). The reaction of CH_3Br with cyclooctene precursors **11** and **12** was not investigated. No reaction between chloromethane and the cyclooctene precursors was observed at room temperature; at higher temperatures (60 → 80 °C), the incipient methyl chloride species is unstable[22] and, as yet, has not been isolated.

These oxidative addition reactions are quite dramatic visually; for example, addition of excess CH_3I to the iridium cyclooctene derivative **6** results in a color change from clear orange to deep emerald green and the isolation of black-green crystals of **14**. Spectacular color changes from yellow-orange to deep green, purple, or blue are observed for all of the reactions depending on the metal, the halide, and the substituents on phosphorus. Such d–d transitions in the visible region appear to be characteristic[23,26] of most five-coordinate molecules with d^6 configurations (formally Rh(III) and Ir(III) metal centers).

Proton NMR spectra (Table I) for the five-coordinate methyl halide complexes **13–18** are very simple, yet informative. The ligand resonances are characteristic of trans disposed phosphine donors due to virtual coupling observed in the methylene (PCH_2Si) region and, in the case of the diphenylphosphino derivatives, widely separated[27] ortho and meta/para resonances in the phenyl region. In all of these derivatives, the observation of two silylmethyl ($Si(CH_3)_2$) singlets of equal intensity at ambient temperatures indicates inequivalent environments above and below the metal–tridentate ligand plane. However, only three complexes, **13**, **14**, and **17**, have the necessary AB quartet of virtual triplets for the methylene protons consistent with this conclusion. The remaining complexes display a simple virtual triplet (**15**, **16**, and **18**). Interestingly, as the temperature is lowered, the triplet pattern observed for the methylene protons of **18** broadens and an AB quartet of triplets is observed at the low-temperature limit. This temperature dependent process may be associated with the backbone of the ligand as it undergoes a conformational flipping on the NMR time scale. The possibility that these five-coordinate methyl halide com-

(22) Heating **6** and excess CH_3Cl in benzene at 80 °C for 12 h generates $Ir(Ph)Cl[N(SiMe_2CH_2PPh_2)_2]$. This unusual C–H activation process is under investigation.
(23) Hoffman, P. R.; Caulton, K. G. *J. Am. Chem. Soc.* **1975**, *97*, 4221–4228.
(24) Ashworth, T. V.; Chalmers, A. A.; Singleton, E. *Inorg. Chem.* **1975**, *24*, 2125–2126.
(25) Crocker, C.; Empsall, H. D.; Errington, R. J.; Hyde, E. M.; McDonald, W. S.; Markham, R.; Norton, M. C.; Shaw, B. L.; Weeks, B. *J. Chem. Soc. Dalton Trans.* **1982**, 1217–1224.
(26) Siedle, A. R.; Newmark, R. A.; Pignolet, L. H. *Organometallics* **1984**, *3*, 855–849.
(27) Moore, D. S.; Robinson, S. D. *Inorg. Chim. Acta* **1981**, *53*, L171–L173.

Table V. Torsion Angles (deg) with Estimated Standard Deviations in Parentheses for $Ir(CH_3)I[N(SiMe_2CH_2P(i\text{-}Pr)_2)_2]$

I-Ir-P(1)-C(1)	-157.6 (3)	C(5)-P(1)-C(4)-C(13)	-171.2 (7)
I-Ir-P(1)-C(4)	89.2 (2)	Ir-P(1)-C(5)-C(14)	-51.2 (8)
I-Ir-P(1)-C(5)	-34.3 (3)	Ir-P(1)-C(5)-C(15)	-176.9 (5)
P(2)-Ir-P(1)-C(1)	90.1 (4)	C(1)-P(1)-C(5)-C(14)	73.2 (8)
P(2)-Ir-P(1)-C(4)	-23.1 (4)	C(1)-P(1)-C(5)-C(15)	-52.5 (7)
P(2)-Ir-P(1)-C(5)	-146.6 (4)	C(4)-P(1)-C(5)-C(14)	-177.0 (7)
N-Ir-P(1)-C(1)	27.2 (3)	C(4)-P(1)-C(5)-C(15)	57.3 (7)
N-Ir-P(1)-C(4)	-85.9 (2)	Ir-P(2)-C(2)-Si(2)	4.8 (6)
N-Ir-P(1)-C(5)	150.6 (4)	C(6)-P(2)-C(2)-Si(2)	139.9 (5)
C(3)-Ir-P(1)-C(1)	-64.6 (4)	C(7)-P(2)-C(2)-Si(2)	-112.9 (6)
C(3)-Ir-P(1)-C(4)	-177.7 (3)	Ir-P(2)-C(6)-C(16)	68.0 (8)
C(3)-Ir-P(1)-C(5)	58.8 (4)	Ir-P(2)-C(6)-C(17)	-68.1 (7)
I-Ir-P(2)-C(2)	-168.3 (4)	C(2)-P(2)-C(6)-C(16)	-56.5 (8)
I-Ir-P(2)-C(6)	68.9 (4)	C(2)-P(2)-C(6)-C(17)	167.4 (6)
I-Ir-P(2)-C(7)	-53.2 (3)	C(7)-P(2)-C(6)-C(16)	-166.6 (7)
P(1)-Ir-P(2)-C(2)	-56.1 (5)	C(7)-P(2)-C(6)-C(17)	57.3 (7)
P(1)-Ir-P(2)-C(6)	-178.9 (4)	Ir-P(2)-C(7)-C(18)	-46.2 (7)
P(1)-Ir-P(2)-C(7)	59.1 (5)	Ir-P(2)-C(7)-C(19)	-172.5 (7)
N-Ir-P(2)-C(2)	6 5 (4)	C(2)-P(2)-C(7)-C(18)	70.2 (8)
N-Ir-P(2)-C(6)	-116.3 (4)	C(2)-P(2)-C(7)-C(19)	-56.2 (9)
N-Ir-P(2)-C(7)	121.6 (4)	C(6)-P(2)-C(7)-C(18)	178.7 (7)
C(3)-Ir-P(2)-C(2)	98.6 (5)	C(6)-P(2)-C(7)-C(19)	52.4 (8)
C(3)-Ir-P(2)-C(6)	-24.2 (4)	C(1)-Si(1)-N-Ir	26.7 (4)
C(3)-Ir-P(2)-C(7)	-146.3 (4)	C(1)-Si(1)-N-Si(2)	-158.5 (4)
I-Ir-N-Si(1)	-92.6 (15)	C(8)-Si(1)-N-Ir	-92.4 (5)
I-Ir-N-Si(2)	92.5 (15)	C(8)-Si(1)-N-Si(2)	82.4 (5)
P(1)-Ir-N-Si(1)	-32.2 (3)	C(9)-Si(1)-N-Ir	146.4 (4)
P(1)-Ir-N-Si(2)	152.8 (3)	C(9)-Si(1)-N-Si(2)	-38.9 (6)
P(2)-Ir-N-Si(1)	156.7 (3)	N-Si(1)-C(1)-P(1)	-2.4 (5)
P(2)-Ir-N-Si(2)	-18.3 (3)	C(8)-Si(1)-C(1)-P(1)	121.0 (5)
C(3)-Ir-N-Si(1)	62.8 (4)	C(9)-Si(1)-C(1)-P(1)	-124.9 (5)
C(3)-Ir-N-Si(2)	-112.2 (4)	C(2)-Si(2)-N-Ir	23.7 (5)
Ir-P(1)-C(1)-Si(1)	-18.3 (5)	C(2)-Si(2)-N-Si(1)	-150.9 (5)
C(4)-P(1)-C(1)-Si(1)	98.3 (4)	C(10)-Si(2)-N-Ir	142.1 (4)
C(5)-P(1)-C(1)-Si(1)	-152.0 (4)	C(10)-Si(2)-N-Si(1)	-32.6 (6)
Ir-P(1)-C(4)-C(12)	-69.9 (3)	C(11)-Si(2)-N-Ir	-96.0 (6)
Ir-P(1)-C(4)-C(13)	54.7 (7)	C(11)-Si(2)-N-Si(1)	89.3 (6)
C(1)-P(1)-C(4)-C(12)	174.7 (4)	N-Si(2)-C(2)-P(2)	-16.7 (7)
C(1)-P(1)-C(4)-C(13)	-60.6 (7)	C(10)-Si(2)-C(2)-P(2)	-140.4 (6)
C(5)-P(1)-C(4)-C(12)	64.1 (4)	C(11)-Si(2)-C(2)-P(2)	104.6 (6)

Table VIII. Final Positional (Fractional, $\times 10^4$; Ir, I, P, and Si, $\times 10^5$) and Isotropic Thermal Parameters ($U \times 10^3$ Å^2) with Estimated Standard Deviations in Parentheses $Ir(CH_3)I[N(SiMe_2CH_2P(i\text{-}Pr)_2)_2]$

atom	x	y	z	U_{eq}
Ir	23967 (2)	25000	40820 (2)	34
I	17908 (7)	16753 (4)	60968 (5)	66
P(1)	3842 (19)	18171 (11)	23853 (18)	42
P(2)	41739 (20)	34085 (12)	56580 (17)	43
Si(1)	21880 (22)	26717 (18)	8877 (17)	47
Si(2)	34673 (24)	42125 (12)	27990 (22)	49
N	2659 (6)	3192 (3)	2465 (5)	42
C(1)	731 (8)	1829 (5)	786 (8)	55
C(2)	4642 (11)	4270 (6)	4682 (9)	69
C(3)	3958 (8)	1561 (5)	4066 (9)	60
C(4)	-1339 (6)	2500	2000 (6)	59
C(5)	-239 (9)	681 (5)	2548 (9)	60
C(6)	6000 (8)	3049 (7)	6916 (9)	66
C(7)	3340 (10)	3967 (5)	6785 (8)	60
C(8)	3781 (10)	2086 (6)	635 (10)	72
C(9)	1402 (11)	3440 (6)	-619 (8)	69
C(10)	4732 (12)	4473 (8)	1859 (10)	89
C(11)	2021 (15)	5106 (6)	2357 (16)	109
C(12)	-1895 (8)	2500	3199 (9)	91
C(13)	-1180 (11)	3393 (7)	1621 (12)	83
C(14)	1032 (12)	37 (6)	2937 (14)	88
C(15)	-1517 (11)	374 (6)	1277 (10)	75
C(16)	7088 (11)	2746 (9)	6202 (12)	96
C(17)	5907 (8)	2500	7992 (8)	90
C(18)	1801 (12)	4341 (7)	5931 (13)	88
C(19)	4344 (15)	4673 (7)	7736 (11)	95

plexes are involved in rapid intramolecular rearrangements between the various isomers in solution was considered; unfortunately, the observed variable-temperature behavior of these complexes (e.g., **18**) is ambiguous with regard to such a process. The low temperature behavior of **15** and **16** was not studied due to the near overlap of the methylene (PCH_2Si) and the methyl ($P(CH(CH_3)_2)_2$) resonances even at 400 MHz.

The above spectral data do not readily distinguish between the two basic geometries for five-coordinate molecules: trigonal bipyramidal (tbp) vs. square pyramidal (sqp). In addition, for the latter case, there is an uncertainty as to which ligand is apical: methyl, sqp1; halo, sqp2; or amido, sqp3. However, most theoretical treat-

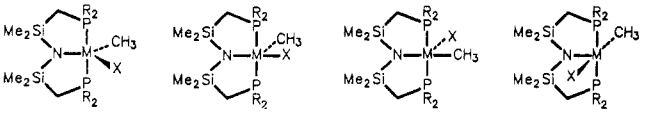

ments[28] of five-coordinate d^6 molecules predict that the square-pyramidal geometry is more stable.[29] Indeed, solution[23,24] and solid-state[25,26,30] studies support this formulation.

Single-crystal X-ray analysis of $Ir(CH_3)I[N(SiMe_2CH_2P(i\text{-}Pr)_2)_2]$ (**16**) indicates a slightly distorted square-pyramidal geometry (Figure 1) with the methyl

(28) (a) Rossi, A. R.; Hoffman, R. *Inorg. Chem.* **1975**, *14*, 365–374. (b) Burdett, J. K. *Inorg. Chem.* **1975**, 375–382. (c) Elian, M.; Hoffmann, R. *Inorg. Chem.* **1975**, *14*, 1058–1076.

(29) If the d^6, five-coordinate molecule contains a single-faced π-donor, e.g. amido, calculations suggest that the more stable geometry is trigonal bipyramidal; see: Thorn, D. L.; Hoffman, R. *Nouv. J. Chim.* **1973**, *3*, 39–45.

(30) Troughton, P. G. H.; Skapski, A. C. *J. Chem. Soc., Chem. Commun.* **1968**, 575–576.

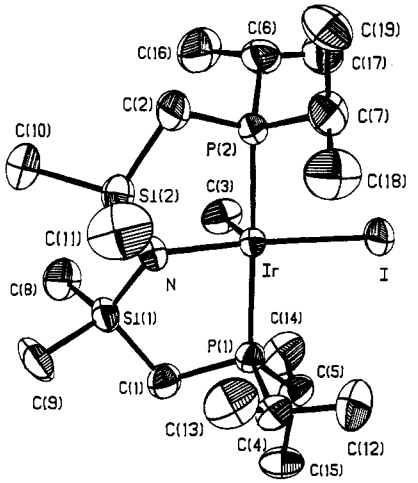

Figure 1. ORTEP drawing of $Ir(CH_3)I[N(SiMe_2CH_2P(i\text{-}Pr)_2)_2]$ (**16**) with thermal ellipsoids at the 50% probability level.

group occupying the apical site (i.e., sqp1). This geometry is quite reminiscent of the solid-state structures found for $Rh(CH_3)I_2(PPh_3)_2$[26] and $Rh(CH_3)I_2(PPh_3)_2{\cdot}C_6H_6$,[30] wherein a square-pyramidal structure with the methyl group apical was also observed. In fact, the iridium atom in **16** sits 0.1441 (1) Å above the least-squares plane defined by N, I, P(1), and P(2) similar to that found in the aforementioned rhodium complexes. The bond lengths (Table III) and bond angles (Table IV) for **16** are unexceptional. Peculiar to **16**, however, is the puckering in the ligand backbone observed in the solid state; the Si_2N plane is tilted with respect to the least-squares plane described above.

The observed solid-state geometry sqp1 is consistent with the solution NMR data; however, as mentioned above so are all the other possible isomers. In the next section, we present convincing arguments to support the sqp1 geometry in solution.

Carbonylation of the Methyl Iodide Derivatives. These coordinatively unsaturated methyl iodide derivatives react immediately with 1 atm of carbon monoxide to give simple, octahedral carbonyl adducts of the general formula $M(CH_3)I(CO)[N(SiMe_2CH_2Pr_2)_2]$ (M = Ir, R = Ph, **19**; M = Ir, R = *i*-Pr, **20**; M = Rh, R = Ph, **21**; M = Rh, R = *i*-Pr, **22**). The intense colors of the starting materials are immediately discharged upon contact with CO to generate pale yellow or yellow-orange solutions of the octahedral carbonyl complexes. The rhodium complexes **21** and **22** are somewhat unstable to loss of CO when exposed to vacuum as evidenced by the gradual return of the color of the starting methyl iodide derivative; this decomposition can be slowed by maintaining an excess of CO over these derivatives in solution and in the solid.

By ^1H and $^{31}P\{^1H\}$ NMR, only one isomer is formed in these reactions. Once again, the presence of virtual coupling for the methylene protons in the ^1H NMR spectrum is consistent with trans phosphine donors, thereby establishing that the tridentate ligand is bound in a meridional fashion on the octahedral complex. This necessarily generates only three possible stereoisomers for the solution structures of these carbonyl adducts: o1; o2; or o3. We

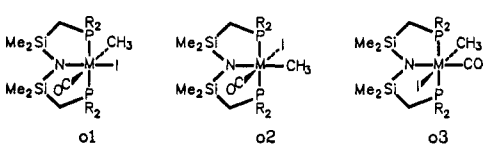

were able to partially distinguish between these isomers by nOe difference experiments.[31] As shown in Figure 2,

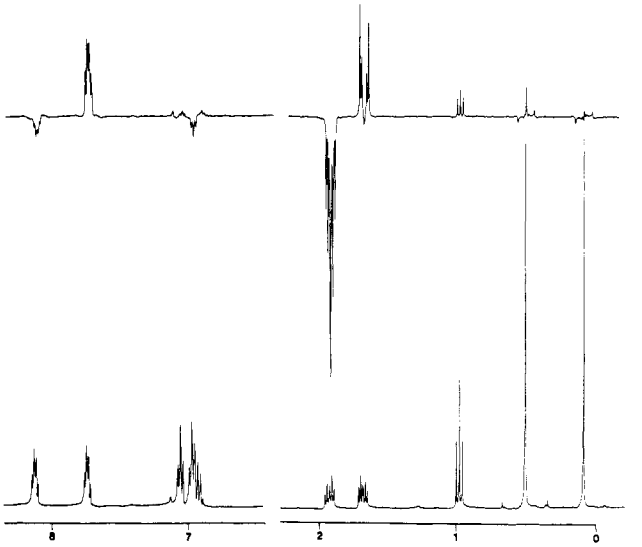

Figure 2. Nuclear Overhauser effect difference experiment for the complex $Ir(CH_3)I(CO)[N(SiMe_2CH_2PPh_2)_2]$ (**19**). Bottom: normal ^1H NMR spectrum. Top: nOe difference spectrum obtained by irradiating the downfield methylene resonance at 1.90 ppm. The enhancement observed for the iridium methyl at 0.95 ppm is indicative of a cis geometry for the methyl and the amide donors. Also noteworthy is the expected enhancement for one set of silyl methyls and one set of ortho protons on the phosphorus phenyls of the ligand backbone.

irradiation of the downfield portion of the methylene protons of **19** results in a significant enhancement of the triplet for the iridium methyl group thus establishing a cis relationship between the amide donor and the methyl ligand; as no enhancement of the methyl resonance is observed when the upfield portion of the methylene resonance is irradiated, isomer o2 with the methyl group trans to the amide is eliminated.

Retrosynthetic considerations suggest that isomer o3 would result from an overall trans oxidative addition of CH_3I to a square-planar derivative of the formula $M(CO)[N(SiMe_2CH_2PR_2)_2]$. In fact, addition of iodomethane to the readily available iridium(I) carbonyl derivative **8** results in the formation of a new carbonyl complex, **23**, which is isomerically pure and distinct (by ^1H NMR and IR spectroscopy) from the corresponding derivative **19**. Given that oxidative addition of alkyl halides proceeds kinetically to generate trans adducts,[32] we assign the stereochemistry of **23** as that depicted by o3 (eq 5).

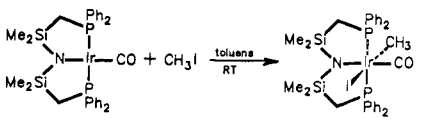

8 23 (5)

Further support for this particular isomeric formulation for **23** is the nOe difference spectrum which indicates that the methyl ligand and the amide donor are again cis as discussed above for **19**. Therefore, by process of elimination, the stereochemistry of **19** is o1. Although this analysis strictly applies only to the iridium derivatives, we feel confident in extending these arguments to all of the carbonyl adducts **19–22**.

The identification of the stereochemistry of these carbonyl adducts as being isomer o1 in turn suggests that the

(31) The nuclear Overhauser effect difference spectra (NOEDIFF) were obtained using standard pulse sequences; see: Saunders, J. K. M.; Mersh, J. D. *Prog. Nucl. Magn. Reson. Spectrosc.* **1983**, *15*, 353.

(32) Collman, J. P.; Hegedus, L. S. *Principles and Applications of Organotransition Metal Chemistry*; University Science Books: Mill Valley, CA; 1980; Chapter 4, pp 185–186.

particular square-pyramidal geometry observed in the solid state, i.e., sqp1, persists in solution; in other words, carbon monoxide adds to the open face of the square pyramid trans to the apical methyl ligand (eq 6). The stereose-

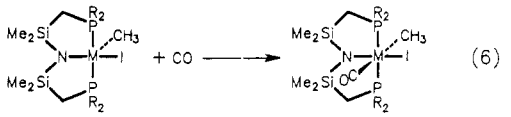

sqp1 o1 (6)

lectivity of the CO addition also tends to exclude the possibility that the five-coordinate methyl halides are involved in stereochemical rearrangements on the NMR time scale as this should lead to the formation of isomeric octahedral[33] carbonyl derivatives.

Notable in these carbonylation reactions of the rhodium and iridium methyl iodides is the absence of any products corresponding to migratory insertion, i.e., acetylmetal complexes. We attribute this to both the unfavorable trans disposition of the methyl and carbonyl ligands in the o1 isomer and the presence of the strongly bound tridentate ligand. This contrasts the behavior[26] of $Rh(CH_3)I_2(PPh_3)_2$ with carbon monoxide for which two isomeric forms of the octahedral acetyl complex $Rh(COCH_3)I_2(PPh_3)_2CO$ are reported.

Conclusions

Amide complexes of rhodium and iridium in both the formal +1 and +3 oxidation levels have now been realized. Undoubtedly, the facility by which these complexes are formed and their resultant stability are due to the incorporation of the amide donor into a chelating array that contains phosphine donors.

The presence of the amide ligand in the coordination sphere does not preclude simple substitution reactions of the corresponding square-planar d^8 derivatives (Rh(I) and Ir(I)), nor does it impede the oxidative addition of certain methyl halides to generate five-coordinate d^6 complexes (Rh(III) and Ir(III)); as both of these types of transformations are part of the arsenal of the synthetic coordination chemist, it would appear that the design of transition-metal-based catalytic systems using amide ancillary ligands is at least viable.

Acknowledgment. Financial support was generously provided by NSERC of Canada and the Alfred P. Sloan Foundation. We also thank Professor James Trotter for the use of his diffractometer and structure solving programs. The generous loan of $RhCl_3$ and $IrCl_3$ from Johnson-Matthey is also acknowledged.

Registry No. **1**, 84074-26-0; **2**, 84074-27-1; **3**, 84074-25-9; **4**, 84074-29-3; **5**, 84074-28-2; **6**, 84074-30-6; **7**, 104835-44-1; **8**, 84074-31-7; **9**, 104835-43-0; **10**, 84074-32-8; **11**, 104835-45-2; **12**, 96110-15-5; **13**, 104848-75-1; **14**, 96110-11-1; **15**, 104835-46-3; **16**, 96110-12-2; **17**, 104835-47-4; **18**, 104293-28-9; **19**, 104835-48-5; **20**, 104835-49-6; **21**, 104835-50-9; **22**, 104835-51-0; **23**, 104874-24-0; $[Rh(\eta^2\text{-}C_8H_{14})_2Cl]_2$, 12279-09-3; $[Ir(\eta^2\text{-}C_8H_{14})_2Cl]_2$, 12246-51-4; $[Rh(CO)_2Cl]_2$, 14523-22-9; $[Rh(\eta^2\text{-}C_2H_4)_2Cl]_2$, 12081-16-2; $Rh(PMe_3)_4Cl$, 70525-09-6; $Rh(PPh_3)_3Cl$, 14694-95-2; $LiN(SiMe_2CH_2P(i\text{-}Pr)_2)_2$, 94372-12-0; $LiN(SiMe_2CH_2PPh_2)_2$, 77617-69-7.

Supplementary Material Available: Tables of intraannular torsion angles and hydrogen coordinates and isotropic thermal parameters (3 pages); a listing of observed and calculated structure factors (19 pages); ordering information is given on any current masthead page.

(33) Kinetically trapping the various five-coordinate isomers by CO would lead to substitutionally inert and configurationally stable derivatives which would be easily distinguished.

The Rhenium Mesityl Oxide Complex $(\eta^5\text{-}C_5Me_5)Re(CO)_2(\eta^2\text{-}Me_2C{=}CHCOMe)$: X-ray Crystal Structure Determination and Solution Isomerism

Frederick W. B. Einstein, Richard H. Jones, A. Hugo Klahn-Oliva, and Derek Sutton*

Department of Chemistry, Simon Fraser University, Burnaby, British Columbia V5A 1S6, Canada

Received April 14, 1986

Reaction of $Cp^*Re(CO)_2(N_2)$ ($Cp^* = \eta\text{-}C_5Me_5$) with $[Me_3O][BF_4]$ or $[Et_3O][BF_4]$ in acetone affords $Cp^*Re(CO)_2(\eta^2\text{-}Me_2C{=}CHCOMe)$ (**8**), which is also obtainable from $Cp^*Re(CO)_2(THF)$ (THF = tetrahydrofuran) and mesityl oxide. The X-ray crystal structure of **8** shows the mesityl oxide to be coordinated through the olefinic group and to be in the s-cis conformation. Compound **8** crystallizes in the space group $P2_1/n$ with $a = 8.515$ (2) Å, $b = 14.277$ (4) Å, $c = 15.093$ (4) Å, and $\beta = 99.30$ (2)°. The structure was solved by using 1885 observed reflections with intensities $I \geq 3\sigma(I)$ in the range $0° \leq 2\theta \leq 48°$ and refined to values of $R = 0.034$ and $R_w = 0.044$. The presence, in solution, of s-cis and s-trans conformers of **8** is indicated by two sets of $\nu(CO)$ absorptions in the IR spectrum (hexane), but the single set of ^1H NMR resonances observed over the temperature range +50 to −80 °C indicates these conformers to be in rapid equilibrium.

Introduction

Reports of transition-metal complexes of mesityl oxide (4-methyl-3-penten-2-one) (**1**) date back to 1840, when Zeise[1] described the platinum complex $C_6H_{10}OPtCl_2$. More than a century later, Parshall and Wilkinson[2] used IR and ^1H NMR results to formulate this platinum compound as a polymer, with $PtCl_2$ units bridged by the mesityl oxide ligand (**1**) using both its olefin and ketone functions. However, much more recently Gillard et al.[3] have reexa-

(1) (a) Zeise, H. *J. Prakt. Chem.* **1840**, *20*, 193. (b) Prandtl, W.; Hofmann, K. A. *Chem. Ber.* **1900**, *33*, 2981.

(2) Parshall, G. W.; Wilkinson, G. *Inorg. Chem.* **1962**, *1*, 896.

0276-7333/86/2305-2476$01.50/0